AD-A052 450 NORTHROP RESEARCH AND TECHNOLOGY CENTER PALOS VERDES --ETC F/G 11/3
OPTICAL COATINGS 2-6 MICRONS.(U)
MAR 78 P KRAATZ N00123-76-C-1321
UNCLASSIFIED NL

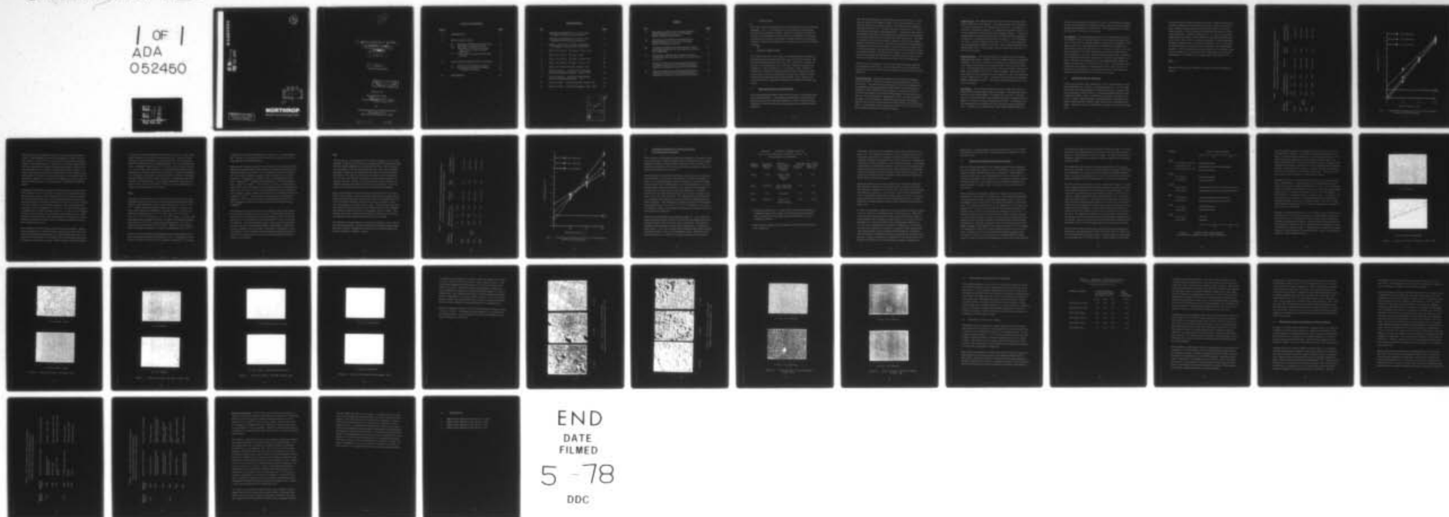

AD A052450

AD No.
DDC FILE COPY

(20)

DDC
RECEIVED
APR 4 1978
F

NORTHROP

Research and Technology Center

DISTRIBUTION STATEMENT A
Approved for public release;
Distribution Unlimited

OPTICAL COATINGS 2-6 MICRONS.

TECHNICAL REPORT,

Mar[illegible]978

45P.

P. Kraatz
Principal Investigator

DISTRIBUTION STATEMENT A
Approved for public release;
Distribution Unlimited

Prepared For

Naval Weapons Center

Contract No. N00123-76-C-1321

By

Northrop Research and Technology Center
One Research Park
Palos Verdes Peninsula, CA 90274

407 696 JOB

TABLE OF CONTENTS

Section		Page
1.0	INTRODUCTION	1
2.0	SINGLE LAYER FILMS	1
	2.1 Deposition Techniques and Optimization	1
	2.2 Absorptance and Film Thickness	4
	2.3 Absorptance and Structure of Single Layer Films on Polycrystalline Substrates	14
	2.4 Effect of HF Vapor Environment Upon Coatings	17
3.0	MULTILAYER ANTIREFLECTION COATINGS	31
	3.1 Absorptance of Multilayer Coatings	31
	3.2 Structure and Preferred Orientation in Multilayer Coatings	34
4.0	REFERENCES	40

ILLUSTRATIONS

No.		Page
1.	Total Optical Absorptance at 3.8 μm Vs. Film Thickness for PbF_2 on SrF_2 Substrates.	7
2.	Total Optical Absorptance at 3.8 μm Vs. Film Thickness for SiO on CaF_2 Substrates.	13
3.	Summary of HF Vapor Tolerance Test Results for Coatings on CaF_2 and SrF_2 Substrates.	19
4.	PbF_2 ($\lambda/2$) on CaF_2 · HF vapor, 30 Min. 167X	21
5.	PbF_2 ($\lambda/4$) on SrF_2 · HF vapor, 305X	22
6.	ThF_4 ($\lambda/2$) on CaF_2 · HF vapor, 30 Min. 167X	23
7.	ThF_4 ($\lambda/4$) on SrF_2 · HF vapor, 30 Min. 167X	24
8.	Al_2O_3 ($\lambda/4$) Typical HF vapor damage, 167X	25
9.	SiO ($\lambda/4$) on CaF_2. Typical HF Vapor Damage on Three Substrate Orientations. 60 Min. 167X	27
10.	SiO ($\lambda/4$) on SrF_2. Typical HF Vapor Damage on Three Substrate Orientations. 167X	28
11.	ZnS ($\lambda/4$) Films. Typical HF Damage 30 Min. 167X	29
12.	ZnSe ($\lambda/4$) Films. Typical HF Damage 15 Min. 167X	30

NTIS Section
DDC Section
UNANNOUNCED
JUSTIFICATION Letter on file
BY
DISTRIBUTION/AVAILABILITY CODES
Dist. SPECIAL
A

TABLES

No.		Page
I.	Absorptance of PbF_2 Films of Integral Halfwave Optical Thickness at 3.8 μm (λ_o) on Oriented Single Crystal SrF_2 Substrates.	6
II.	Absorptance of SiO Films of Integral Halfwave Optical Thickness at 3.8 μm (λ_o) on Oriented Single Crystal CaF_2 Substrates.	12
III.	Comparison of Single Layer Film ($\lambda_o/2$ at 3.8 μm) Absorption Coefficients on Single and Polycrystalline CaF_2 Substrates.	15
IV.	Absorptance of Antireflection Coatings on Single Crystal CaF_2 and SrF_2 Substrates (2 coated surfaces) at 3.8 μm).	32
V.	Summary of Structures and Preferred Orientation in Component Films of the ThF_4/PbF_2 Quarterwave-Quarterwave Coating on CaF_2 and SrF_2 Substrates.	35
VI.	Summary of Structures and Preferred Orientation in Component Films of the ThF_4/SiO Quarterwave-Quarterwave Coating on CaF_2 and SrF_2 Substrates.	36

1. INTRODUCTION

This report covers the final half-year of the contractual effort (June through December, 1977). It is divided into two major sections covering single layer films and multilayer coatings. Deposition techniques and their optimization, film absorptance, film structure, and resistance to an HF vapor environment are covered in the section on single layer films; absorptance, structure, and preferred orientation are covered in the section on multilayer coatings.

2. SINGLE LAYER FILMS.

The results of the most recent efforts at optimizing deposition conditions and characterizing the single layer films are covered in this section. Deposition techniques optimized for ThF_4, PbF_2, SiO, ZnS, and ZnSe are covered in some detail in the first subsection. Results of studies of absorptance vs. film thickness (βL vs. L) for PbF_2, ThF_4, and SiO are covered next, followed by results detailing effects of polycrystalline substrates upon structure and absorptance of single layer coatings. Results of exposure of single layer film materials (PbF_2, ThF_4, Al_2O_3, SiO, ZnS, and ZnSe) to a humid HF environment are presented in the final subsection.

2.1 Deposition Techniques and Optimization

Any coating optimization effort requires careful control of evaporation techniques and parameters. A complicated interdependence exists among deposition parameters and thin film properties, so that one property may be influenced by several conditions and one parameter may influence several properties.

All of the coating depositions described in this report were done in a commercial coating system (Balzers Model 710) which was pumped by an oil diffusion pump and a liquid nitrogen trap. The system was evacuated to a pressure of less than 10^{-6} Torr and a pressure of less than 5×10^{-6} Torr was maintained during the coating depositions. To ensure the uniformity of the thickness of the layers, the samples were rotated above the evaporation source (approximately 30 inches) during the deposition process. The mode of evaporation was either by resistance heating or electron beam heating. Proper control of the thickness of each layer was afforded by monitoring the reflectance at the control wavelength of a suitably positioned witness plate in the coating chamber and stopping deposition when the reflectance reached a predetermined value. Before placing the sample into the system for coating, they were cleaned by washing with a detergent and warm water, then rinsed with distilled water and alcohol and blown dry with nitrogen gas.

Parameters used to deposit each of the most promising coating materials are described in detail below. All of the materials were purchased from commercial sources, and no attempt was made to further purify any of these materials.

Thorium Fluoride. The starting material for these films was granular thorium fluoride (99.9% purity) purchased from the Balzers High Vacuum Corporation. The material was evaporated by electron-beam heating, and an evaporation rate of approximately 1800Å/Min was used throughout the deposition. Films deposited at lower substrate temperatures ($< 100°C$) showed the appearance of hydroxyl absorption bands at 2.8 µm and 6.2 µm, whereas, for films deposited at approximately 200°C, the hydroxyl absorption bands were not observed. Thorium fluoride deposits as a strongly adherent film having an average refractive index of about 1.49 for the 2-6µm region. Increasing the residual gas pressure from 5×10^{-6} to 1×10^{-5} Torr had no apparent influence on the refractive index.

Lead Fluoride. The coating material for these films was purchased from Balzers High Vacuum Corporation. The material comes as fused granules ($\sim$ 4 mm) of lead fluoride with a stated purity of 99.99%. Lead fluoride is reduced by hot tantalum, tungsten, or molybdenum evaporation sources. It is best evaporated by using electron-beam heating techniques. To assure a constant rate of evaporation, and to avoid overheating and decomposition of the material, a defocused electron-beam of at least 1.5 - 2 cm in diameter was used. A vacuum pressure of less than 5×10^{-6} Torr and a deposition rate of approximately 1800Å/min was used. The substrate temperature was approximately 200°C. The average refractive index of the films was 1.73 for the 2-6 μm region.

Silicon Monoxide. The silicon monoxide was evaporated from a tantalum baffled-box type source, available from R. D. Mathis Company, Long Beach, California. This source produced less spattering of silicon monoxide particles than the electron gun, and resulted in films which were more defect free. The starting material was lumps of Linde select grade of silicon monoxide, also available from the R. D. Mathis Company. True silicon monoxide films can only be prepared by fast evaporation ($>$ 30Å/sec) under good vacuum conditions ($< 10^{-6}$ torr). The films were deposited onto substrates heated to approximately 200°C. The average refractive index was 1.75 for the 2-6 μm region.

Zinc Sulfide. The starting materials for the zinc sulfide films were purchased from the Balzers High Vacuum Corporation. This material came in the form of hot-pressed tablets. The stated purity was 99%. Consistent data for the zinc sulfide films were obtained only after the material was preheated in a vacuum for an hour at approximately 900°C. The material was then evaporated from a tantalum box source having a perforated tantalum cover. The films were evaporated at a rate of approximately 1800Å/min

and at a vacuum pressure less than 5×10^{-6} torr. For maximum durability, the films were deposited on substrates freshly cleaned by a glow discharge and held at temperatures of around 150°C. The average refractive index of the films was 2.25 for the 2-6 μm region.

Zinc Selenide. The starting material for the zinc selenide films was random lumps of CVD zinc selenide obtained from the Raytheon Research Division. In this form, the starting material is dense and no preheating or outgassing is required. The material was evaporated from a tantalum box source having a perforated tantalum cover. Care must be taken not to overheat the material. The source temperature should be just high enough to cause evaporation to proceed, otherwise some alteration in the composition of the material will take place resulting in an increase in absorption in the films. The films were evaporated at a rate of approximately 1000Å/min and at a vacuum pressure of less than 5×10^{-6} Torr. The substrates were maintained at a temperature of approximately 150° C and just prior to deposition they were cleaned by an argon glow discharge. The average refractive index of the films was 2.4 for the 2-6 μm region.

2.2 Absorptance and Film Thickness

In a previous technical report (September, 1977), some advantages of measuring absorptance as a function of coating thickness (βL vs. L) for single layer films of selected materials were discussed briefly in connection with some preliminary results for PbF_2. These measurements have now been completed for PbF_2, ThF_4, and SiO films at a design wavelength (λ_0) of 3.8 μm. Results, and particularly, statistical features, are quire encouraging for PbF_2 and SiO, tending to lend credence to the methodology employed. Results for ThF_4 are problematic, pointing out the need for further work.

The experimental procedure employed for all three coating materials and substrate orientations involved choosing a group of single crystal CaF_2 or SrF_2 substrates having absorptance values falling within a very narrow range (typically 10-15%) to minimize this potential contribution to experimental dispersion. Coatings of thickness $\lambda_o/2$, λ_o, and $3\lambda_o/2$ were then deposited on three groups of three substrates, each group comprising one each of (100), (110), and (111) substrate orientation. Identical deposition conditions (deposition rates, substrate temperatures, etc.) were utilized for all three groups of substrates (film thicknesses) within experimental feasibility. Glow discharge cleaning of substrates was not employed in any of these coating runs in order to minimize complications associated with that operation, as detailed in the technical report dated January, 1977.

$\underline{PbF_2}$–

Results for PbF_2 on SrF_2 substrates are listed in Table I and plotted in figure 1.

Table I. Absorptance of PbF_2 films of integral halfwave optical thicknesses at 3.8 μm (λ_o) on oriented single crystal SrF_2 substrates.

Substrate Orientation	Total Absorptance for Film Thickness of: (10^{-4})				Intercept	Slope (10^{-4})	Film Absorption Coefficient, β (cm^{-1})
	0	$\lambda_o/2$	λ_o	$3\lambda_o/2$			
(100)		3.55	4.91	7.53	1.35 ± 1.80	1.99	1.63 ± 0.17
(110)	1.01 ±0.15	1.99	4.92	6.90	-0.30 ± 0.08	2.45	2.01 ± 0.13
(111)		2.55	4.56	7.29	0.06 ± 0.02	2.37	1.94 ± 0.10
Mean		2.70	4.80	7.24	0.37 ± 2.27	2.27	1.86 + 0.20

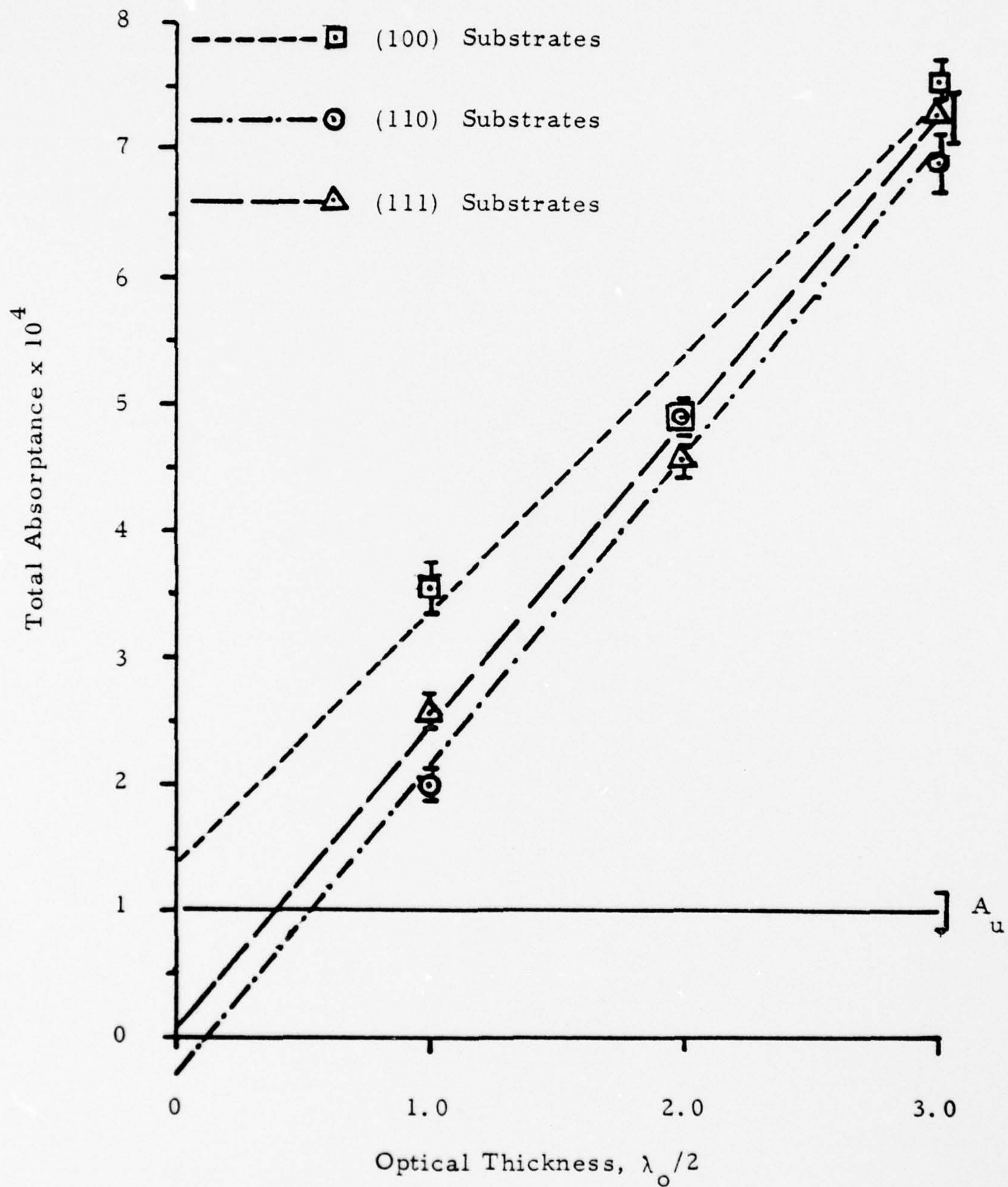

Fig. 1 Total Optical Absorptance at 3.8 µm vs. Film Thickness for PbF_2 on SrF_2 Substrates.

The Miller indices of substrate surfaces are given in the first column of Table I. Total absorptance values for the samples are listed in the next four columns in units of 10^{-4}; the mean value for the uncoated substrates appears in the column headed "0" and values for substrates with halfwave, full wave, and one-and-one-half wave optical thicknesses of PbF_2 at a design wavelength of 3.8 μm appear in appropriately labeled columns. Results of least squares analyses of the absorptance for each substrate orientation appear in the next two columns of the table, with the final result, the absorption coefficient of the thin film (cm^{-1}) appearing in the last column. The least squares lines for all three substrate orientations are plotted in figure 1.

Comparing the absorption coefficients of Table I with our previous data for PbF_2 (September, 1977) shows that the mean value for all substrate orientations has been reduced by more than a factor of two, differences among the substrate orientations have been substantially reduced, and precision has been improved. Absorption coefficients (β) for PbF_2 films on (110) and (111) SrF_2 substrates are essentially identical within experimental error, while that on (100) is significantly (~17%) lower. Our previous data showed a similar trend, but $\beta(100)$ was approximately $1/2\ \beta(110) \leq \beta(111)$. Probable reasons for these changes include improved measurement accuracy, based on three uncoated and coated substrate absorptance determinations for each absorption coefficient and better control of deposition conditions over the three coating runs involved.

The intercepts of the least squares plots deserve some comment. Ideally, plots of absorptance vs. coating thickness should intersect the y-axis at the uncoated substrate absorptance value, A_u, within experimental error, provided that the absorptance of the substrate does not change appreciably from the measured value prior to coating. Positive changes would be associated

with increases in total absorptance and intercept of the βL vs. L plot, while negative changes would result in intercepts below A_u. Changes of either sign could result from exposure to ambient atmosphere or vacuum baking at 200°C immediately prior to coating deposition. For two of the three substrate orientations considered here (110) and (111), the intercepts of the βL vs. L line for PbF_2 falls well below A_u, indicating that substrate surface absorptance is markedly reduced prior to coating. (No physical significance is to be attached to the negative intercept for the (110) substrate orientation; it simply indicates that the surface absorptance is substantially reduced by processes preceding coating, so that substrate absorptance approaches intrinsic levels.) For the (100) surface of SrF_2 the surface absorptance apparently increases slightly prior to coating.

<u>ThF_4</u>–

Absorptance measurements for this material were carried out using a methodology and procedures identical to those successfully employed for PbF_2 and SiO. Mean absorptance of the uncoated substrates was $(1.50 \pm 0.21) \times 10^{-4}$. Coated substrate absorptance results were erratic, showing a tendency toward higher total absorptance for thinner films, e.g. for the (100) substrate orientation, $A(\lambda_o/2) = 7.11 \times 10^{-4}$, $A(\lambda_o) = 4.61 \times 10^{-4}$ and $A(3\lambda_o/2) = 4.61 \times 10^{-4}$ and $A(3\lambda_o/2 = 5.27 \times 10^{-4}$, where $\lambda_o = 3.8\ \mu m$. The mean absorption coefficient $(\bar{\beta})$ for the $(\lambda_o/2)$ films on all substrate orientations was $4.00 \pm 0.23\ cm^{-1}$, that for the λ_o films was $1.51 \pm 0.31\ cm^{-1}$, and that for $3\lambda_o/2$ films was $0.93 \pm 0.4\ cm^{-1}$. Mean $\bar{\beta}$ for all the films on all three substrate orientations, irrespective of thickness, was $2.15\ cm^{-1}$.

This last result may be fairly representative of the average behavior of the films on alkaline earth fluoride substrates at 3.8 µm. Comparison with our previous results for the ThF_4 on SrF_2 reported in September, 1977, shows

a reduction in the average absorptance by a factor of 1.7 or approximately 40%. However, the uncertainty in the results is much greater, due to the large differences with film thickness.

Detailed x-ray diffraction analyses of the ThF_4 films for all substrate orientations and film thicknesses showed sharp and consistent differences correlating with substrate orientation, but no systematic changes with film thickness on any single substrate orientation. On (100) SrF_2, ThF_4 is microcrystalline with spacings of 2.02Å and 3.80Å, corresponding to (103) and (220), respectively[1]. An additional sharp peak at 3.21Å is attributable to $ThF_4 \cdot nH_2O$[2] or $ThOF_2$[3]. On (110) SrF_2, the ThF_4 is entirely amorphous with no diffraction maxima except those arising from the uncoated substrate. On (111) SrF_2, ThF_4 is well crystallized with very strong preferred orientation, showing a single diffraction peak corresponding to (322) with a spacing of 1.85Å[1]. A second sharp diffraction peak corresponding to a spacing of 1.235Å could be attributed to an uncataloged ThF_4 line, but is more probably associated with a hydrated phase (the (640) line of $ThF_4 \cdot 0.88H_2O$)[4].

The possible presence of hydrated ThF_4 or Thorium oxides would account for the higher absorptance values at 3.8 µm. The evaporant starting material is the most probable source of these impurities. However, the apparent decrease in absorptance with increased film thickness is not so easily explained. A possible mechanism which could account for these observations would involve film defects (pinholes, stacking faults, dislocation pile-ups, vacancies, etc.) as primary contributors to absorptance. If the concentration of these decreases with increasing film thickness (this is unlikely for the thicknesses involved here), then the absorptance would decrease, as is observed.

SiO

Results of βL vs. L experiments involving silicon monoxide films on oriented single crystal CaF_2 substrates are presented in Table II and figure 2 (the format is exactly analogous to that employed with PbF_2, Table I, figure 1). It is immediately clear that the slopes of the plots, and hence the thin film absorption coefficients, are significantly different for the three substrate orientations. This deviates from previous results reported in September, 1977, wherein little influence of substrate orientation upon absorption coefficient was noted. However, the precision of the present results is undoubtedly higher and the statistical parameters are excellent, with the exception of the intercept of the plot for the (110) substrate orientation.

Again, the intercepts for all three substrate orientations are worth noting. On the (100) substrates, surface absorptance apparently decreases to about half the previously measured uncoated value prior to coating deposition. On (110) it increases moderately (but with a very large uncertainty), and on (111) it increases by more than a factor of two. These results are in startling contrast to those for SrF_2 (Fig 1 and Table I) wherein (100) substrates were unique in showing an increase in absorptance prior to coating. This indicates that surface chemistry and absorptance changes prior to and during coating are poorly understood and further work is needed.

The absorptance results themselves are quite encouraging, both in terms of their absolute magnitude, and their relatively high precision, again indicating that the method of comparing film thickness with total absorptance can produce meaningful, consistent, results.

Table II. Absorptance of SiO films of integral halfwave optical thicknesses at 3.8 μm (λ_o) on oriented single crystal CaF_2 substrates.

Substrate Orientation	Total Absorptance for Film Thickness of: (10^{-4})				Intercept (10^{-4})	Slope (10^{-4})	Film Absorption Coefficient, β (cm^{-1})
	0	λ_o	λ_o	$3\lambda_o/2$			
(100)		3.41	6.09	8.87	0.67 ± 0.05	2.73	2.25 ± 0.014
(110)	1.13 ±0.11	3.86	4.89	7.69	1.65 ± 2.01	1.91	1.58 ± 0.24
(111)		3.92	5.31	6.51	2.65 ± 0.12	1.30	1.07 ± 0.03
Mean		3.73	5.43	7.69	1.66 ± 0.99	1.98	1.63 ± 0.60

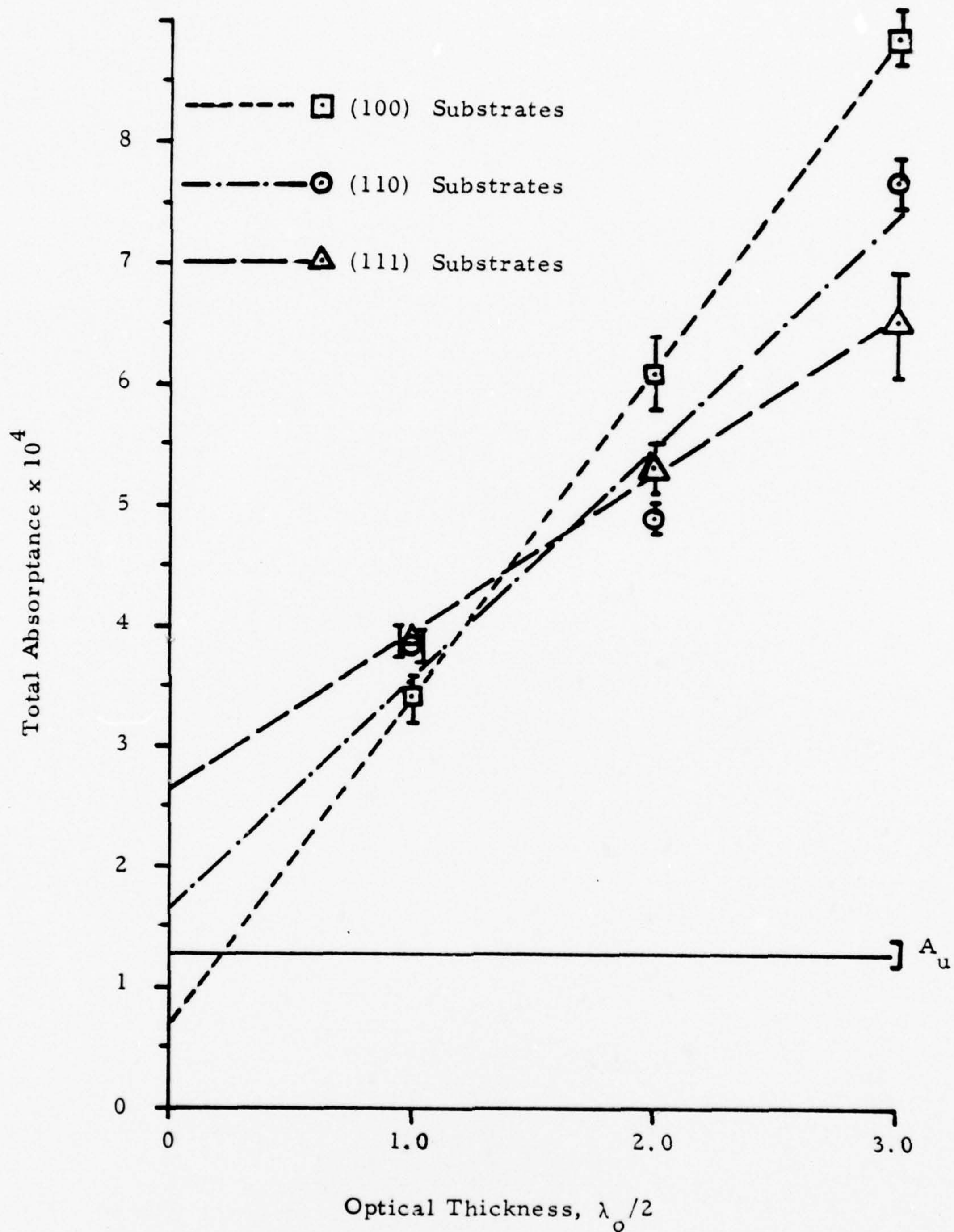

Fig. 2 Total Optical Absorptance at 3.8 μm vs. Film Thickness for SiO on CaF_2 Substrates.

2.3 Absorptance and Structure of Single Layer Films on Polycrystalline Substrates.

Since it has been established that significant differences in absorption coefficient and structure of optical coatings arise from differences in the crystallographic orientation of single crystal substrates, it was necessary to determine these properties for films on polycrystalline substrates, where orientation of individual grains may vary.

Polycrystalline CaF_2 substrates produced by press forging were employed to test this effect. Grain size in this material, produced by Harshaw, is large (~1 cm), but birefringlace effects are minimal. Preferred orientation in a central area of approximately 2 cm^2 was determined by x-ray diffraction before coating the substrates (1 inch diameter) and absorptance of the same area was measured using DF laser calorimetry. A majority (seven of ten) substrates exhibited strong (110) preferred orientation, with minor (311), (111), and (331) peaks. Two substrates showed predominant (111) orientation with subequal (110) and one showed an indeterminate high index orientation. Total absorptances (surface and bulk) at DF wavelengths were generally high, of the order of 10^{-3} cm^{-1} for samples ~0.5 cm thick. No systematic variation of absorptance with preferred orientation of the substrate grains was established.

Results of this investigation are presented in Table III. Four coating materials showing particular promise for the DF laser wavelength region were selected; they are listed in the first column of the table. The preferred orientation of the substrate is given in the second column. A single set of Miller indices, e.g. (110), indicates that the substrate grains had a common orientation parallel to only one crystallographic plane. Where two sets of indices are given, e.g. (110)/(311), the first set indicates the dominant

Table III. Comparison of Single Layer Film ($\lambda_o/2$ at 3.8 μm) Absorption Coefficients on Single and Polycrystalline CaF_2 Substrates.

Coating Material	Polycryst. Subst. Pref. Orient.	Film Struct. & Pref. Orient on Polycryst. Substrate	Film Abs. Coef. (cm^{-1}) Poly Cryst. Substrate	Singl. Cryst. Substrate *
PbF_2	(110)	Cubic (β) (110); Minor (111), Pb_2O_3	2.64	3.03
ThF_4	(110)/(311)	Microcrystalline Monocl. (220)/(103)	1.07	1.65
SiO	(110)	Amorphous	5.37	1.58
ZnSe	(110)/(111)	Cubic (111); Minor $ZnSeO_4$	1.58	1.55**

* Absorption Coefficient for a coating of the same material deposited in a separate coating run on a single crystal CaF_2 substrate having the same orientation as the dominant preferred orientation in the polycrystalline substrate.

** ZnSe coatings on single and polycrystalline substrates deposited in the same coating run.

orientation, with the second set denoting a less strongly preferred set of planes (i.e. lower intensity of diffracted x-rays). Predominant features of the structure and preferred orientation of the halfwave film on the polycrystalline substrate are summarized in the third column and its absorption coefficient at the DF wavelength is given in the fourth column. For purposes of comparison, an absorption coefficient of the film material deposited on a single crystal CaF_2 substrate having the same orientation as the dominant orientation of the polycrystalline sample is listed in the fifth column. (In all cases except that of ZnSe, this number is generated from material deposited during a different coating run).

Agreement between the absorption coefficients of the films on single and polycrystalline substrates is reasonable for three of the four materials, with differences ranging from 2% to about 35%, the value for the polycrystalline substrates being lower, in most cases. Since the total experimental error in the film absorption measurements ranges from 5% to 15%, this degree of agreement is satisfactory and indicates that there are no special problems in extending results on single crystal substrates to the polycrystalline case.

For SiO, the absorption coefficient on the polycrystalline substrate is about 2.5 times that on the corresponding single crystal substrate. Differences in film structure cannot account for this, since all SiO films on single or polycrystalline CaF_2 substrates oriented parallel to (110) have been found amorphous to x-ray in the present work. An absorption coefficient of 5.74 cm^{-1} was reported under this program in September, 1977 for SiO on a (110) SrF_2 substrate; x-ray diffraction analyses of that material indicated small amounts of well crystallized SiO_2 (Tridymite) in addition to microcrystalline and amorphous material, suggesting that the film was oxygen-rich. Evidence supporting this explanation of the high absorption coefficient of the SiO film on the polycrystalline substrate is lacking in the

present case. If excess oxygen is present in the latter film, x-ray diffraction provides no indication that it is incorporated in a crystalline or microcrystalline form.

2.4 Effect of HF Vapor Environment Upon Coatings.

Since the ultimate applications of the coating materials being investigated here are in multilayer coatings for use in HF/DF lasers, the compatibility of these materials with HF vapor must be established. While actual life testing in an HF laser is most representative of service conditions, it is too time-consuming and cost-ineffective for screening and ranking a variety of coating materials. To accomplish such a screening and ranking in the present program, a simple, rapid, cost-effective, but quite severe test was devised.

Thirty-five samples comprising single layer coatings on CaF_2 and SrF_2 substrates (1 inch diameter) were placed in a vinyl container approximately 14 inches in diameter and 7 inches high (approximate volume 17,000 cm^3) with plexiglas cover, maintained in the ambient atmosphere of a fume hood at 21.2°C. A polypropylene beaker (65 mm. diameter x 35 mm. height) containing 50 cm^3 of semi-conductor grade HF was placed in the center of the container above the level of the samples at commencement of the test. A second polypropylene beaker (70 mm. diameter x 90 mm. height) containing 100 cm^3 de-ionized water (initial pH 4.5) was also placed in the large vinyl container prior to the test to provide a pH reference and constant humidity during the test. Final pH of the water was 2.9 at a temperature of 19.5°C. Initial hydrogen ion concentration in the water was thus 3.16×10^{-5} changing to a final value of 1.26×10^{-3}, or an increase by a factor of 40 within 1.25 hours. Samples were observed continuously through the plexiglas cover throughout the test; the cover was removed for approximately 2 minutes every 15 minutes to permit close examination and removal of failed samples.

The criterion for failure was destruction of the physical integrity or optical uniformity of the coating either by crazing and cracking, fogging (general attack), or localized attack at defects or edges. An optical transmission or absorption criterion was not used due to the time required for performance of the test itself.

The coating materials chosen for testing included PbF_2, ThF_4, Al_2O_3, SiO, ZnS, and ZnSe. All but one of these materials (Al_2O_3) exhibits moderate absorptance at 3.8 μm and is thus a preferred candidate coating material. Al_2O_3 was tested in spite of its high 3.8 μm absorptance due to its potential usefulness in the HF laser band (2.7 μm) and in the ultraviolet.

Results of the HF vapor tolerance test are summarized in figure 3. In general, it appears that the oxides are most resistant to outright destruction in the humid HF environment, while the selenides are least resistant. Fluorides and zinc sulfide fall into an intermediate category, with the sole exception of a single quarterwave PbF_2 coating on SrF_2 (100). The latter result was probably fortuitous. With respect to the oxides, the solid lines indicate the time elapsed during formation of a very thin film at the exposed surface; this film exhibited interference rings in the visible and was not removable by solvent cleaning, but microscopic examination showed no evidence of attack of the coating so that it was not considered to have failed at this point. The dashed lines indicate the time elapsed from formation of the thin interference film until destructive effects became evident under the microscope. Here a criterion for failure involving optical transmission or absorption in the 3.8 μm wavelength region would have been more useful.

Modes of failure differed widely among the various coating materials and thicknesses, from general attack (ZnSe, ZnS, SiO, PbF_2) to selective attack at coating defects only (Al_2O_3 and $\lambda/4$ ThF_4 on SrF_2) or characteristic crazing patterns ($\lambda/2$ ThF_4 on CaF_2). Typical damage to PbF_2 films

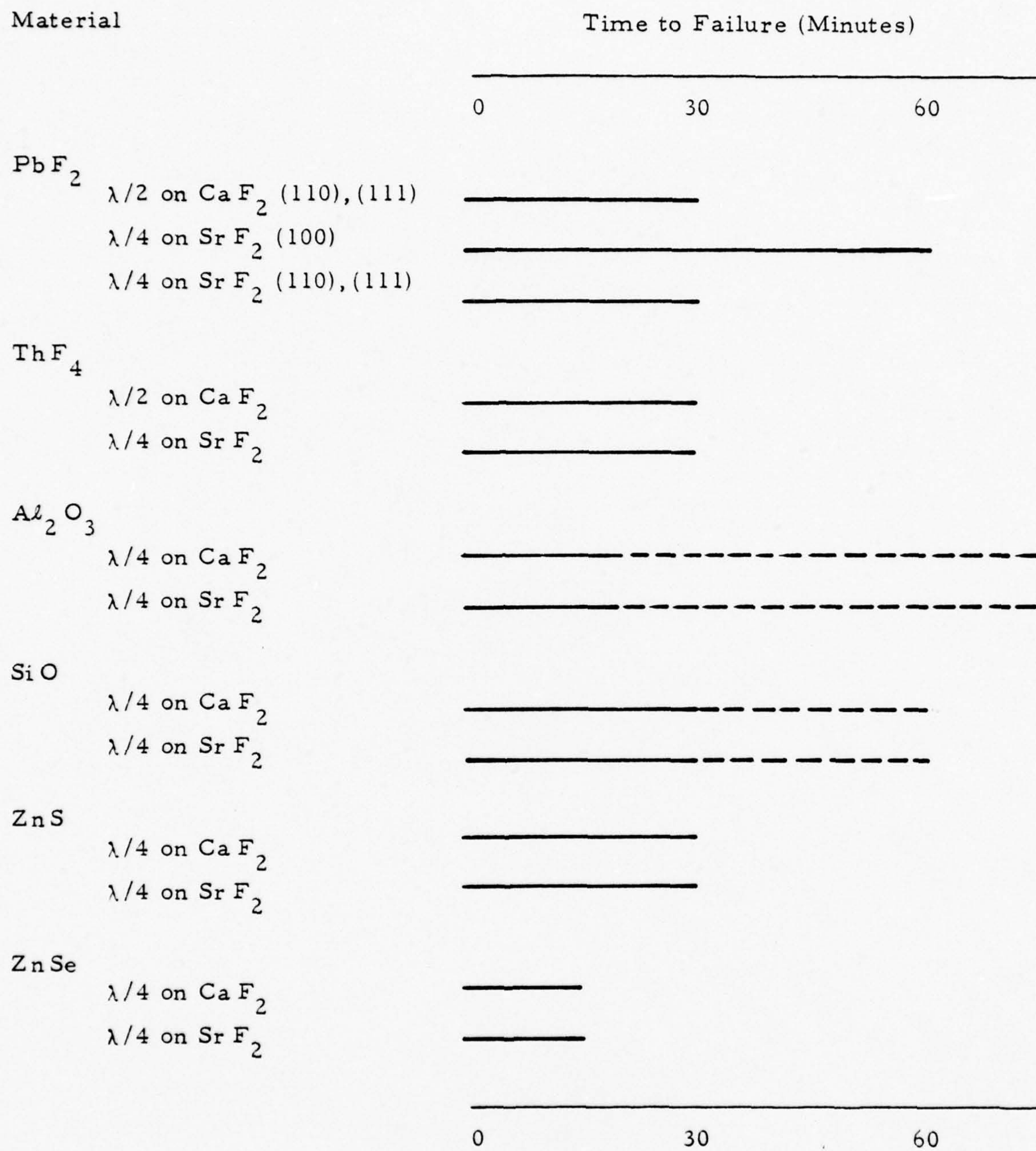

Figure 3. Summary of HF Vapor Tolerance Test Results For Coatings on CaF_2 and SrF_2 Substrates.

on CaF_2 and SrF_2 surfaces is illustrated in figures 4 and 5 respectively. The nature of the damage is etch pitting resulting from general chemical attack. Note the surficial expression of a substrate grain boundary in 4 (a) and the undisturbed appearance of the uncoated substrate surface in the lower half of figure 4 (b). Figure 5 (a) illustrates typical morphology of the damaged PbF_2 surface on (110) and (111) SrF_2 substrates after 30 minutes exposure to the humid HF environment. Figure 5 (b) shows the coating on (100) SrF_2 after 60 min. in the identical environment. The attack in the latter case is just as extensive, but not nearly as severe.

Damaged ThF_4 films are shown in Figures 6 and 7 after 30 minutes exposure to the HF vapor. A characteristic spiral crazing pattern which develops on ThF_4 films of halfwave thickness (at 3.8 or 5.3 μm) on (100) and (110) CaF_2 surfaces is illustrated in Figure 6 (a) while more general attack typical of the (111) surface is illustrated in figure 6 (b). HF damage to ThF_4 *films of* $\lambda/4$ *thickness on* SrF_2 *is shown in figure 7.* Crazing is conspicuously absent in all cases, the damage comprising pits and blisters, probably initiating at defects in the original coating. Thus there is an apparent substrate material and/or film thickness dependence for damage to ThF_4 films by wet HF vapor.

Damage to quarterwave thickness (at 3.8 μm) Al_2O_3 films is similar for all orientations of CaF_2 and SrF_2 substrates, comprising highly localized attack at film defects, surrounded by altered surficial material exhibiting a concentric ring interference pattern, similar to the microscopic pattern described above in connection with the onset of damage to these films. Typical examples are shown in Figure 8. Apparently, the mechanism of damage remains the same throughout the exposure period, simply progressing more rapidly at certain widespread defects.

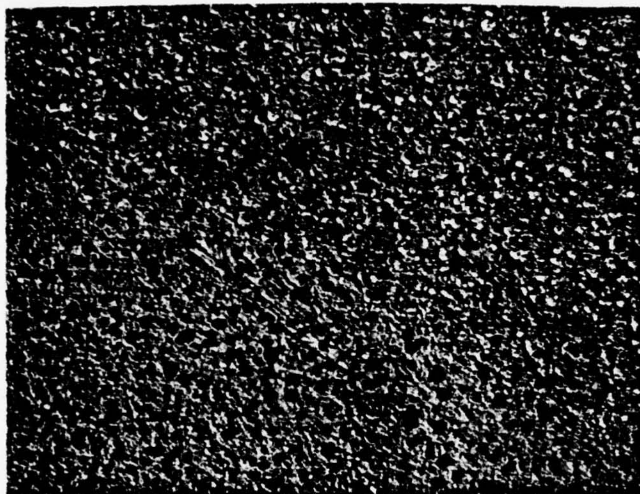

a) (110) Surface

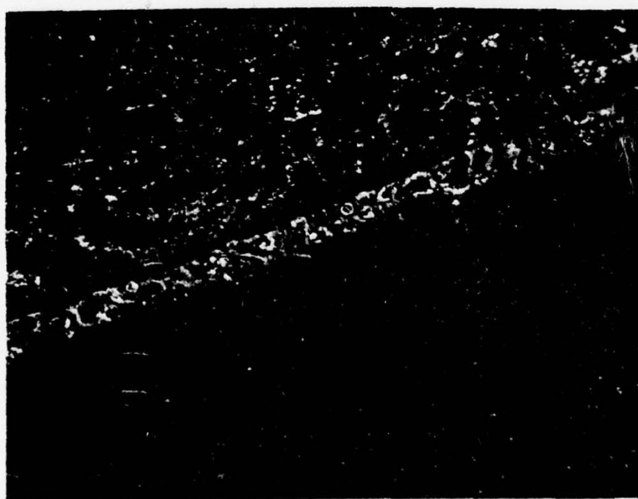

b) (111) Surface, Coating Edge.

Figure 4. PbF_2 ($\lambda/2$) on CaF_2 · HF vapor, 30 Min. 167X.

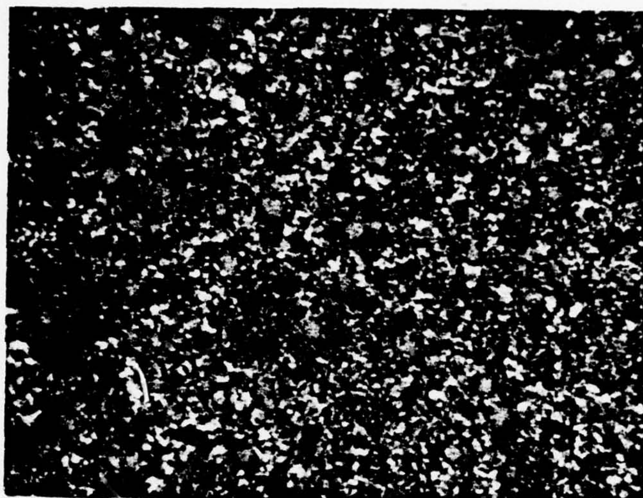

a) (110) Surface 30 Min.

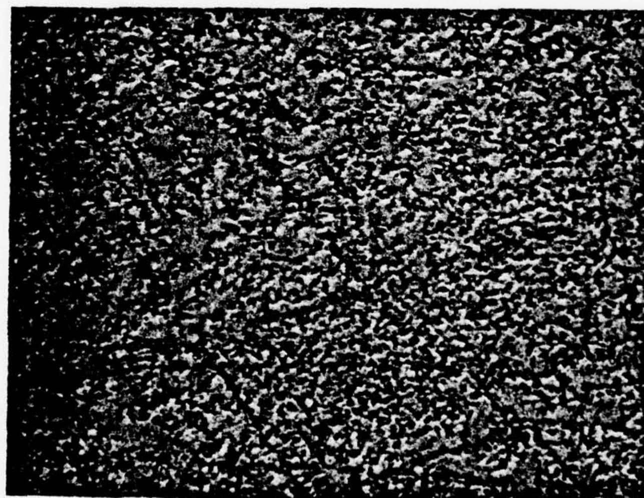

b) (100) Surface 60 Min.

Figure 5. PbF_2 ($\lambda/4$) on SrF_2 · HF vapor, 305X

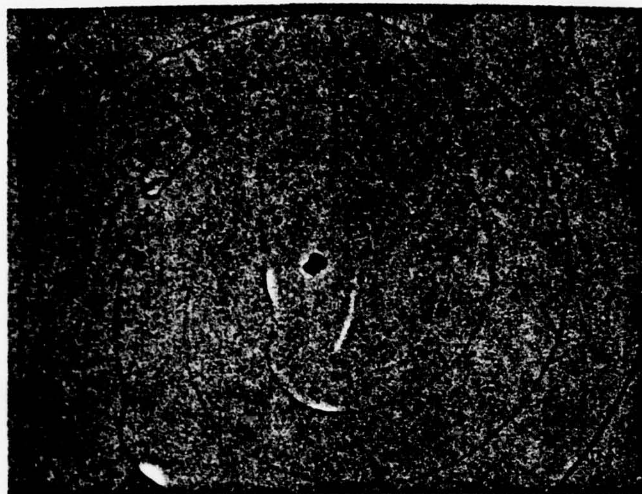

a) (100) Surface

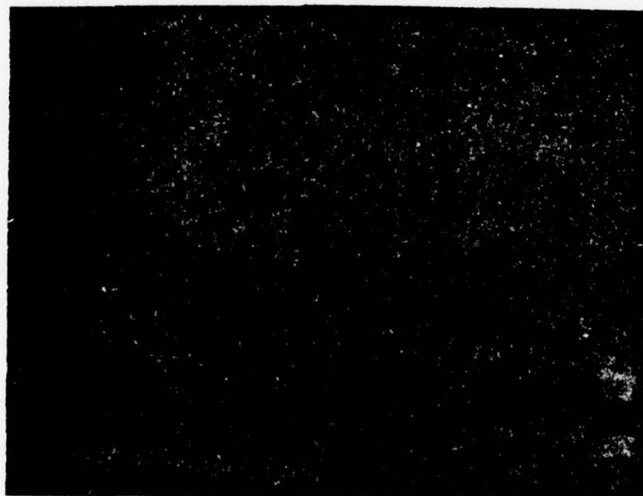

b) (111) Surface

Figure 6. ThF_4 ($\lambda/2$) on CaF_2 · HF vapor, 30 Min. 167X.

a) (110) Surface, Center, Tylical.

b) (110) Surface, Near Edge, Atypical Area.

Figure 7. ThF_4 ($\lambda/4$) on SrF_2 · HF vapor, 30 Min. 167X.

a) CaF_2 (100) Substrate

b) SrF_2 (111) Substrate

Figure 8. Al_2O_3 ($\lambda/4$) Typical HF vapor damage, 167X.

A comparison of morphology and severity of HF vapor damage to SiO films on three orientations of CaF_2 and SrF_2 is given in figures 9 and 10. The least severely damaged SiO films appear on (111) CaF_2 surfaces and on (100) SrF_2 surfaces. The SiO films are most amorphous on these substrate orientations, exhibiting no diffraction peaks attributable to well crystallized SiO_2. Also, probably fortuitously, SiO films have their lowest absorption coefficients on (111) CaF_2 substrate surfaces. Thus we may tentatively conclude that amorphous SiO films are more resistant to HF vapor attack than films composed of measurable amounts of crystalline SiO_2.

Typical HF damage morphology in ZnS and ZnSe quarterwave films is shown in figures 11 and 12. The damage mechanism appears to be relatively uniform chemical attack, with no systematic differences correlating with substrate composition or orientation.

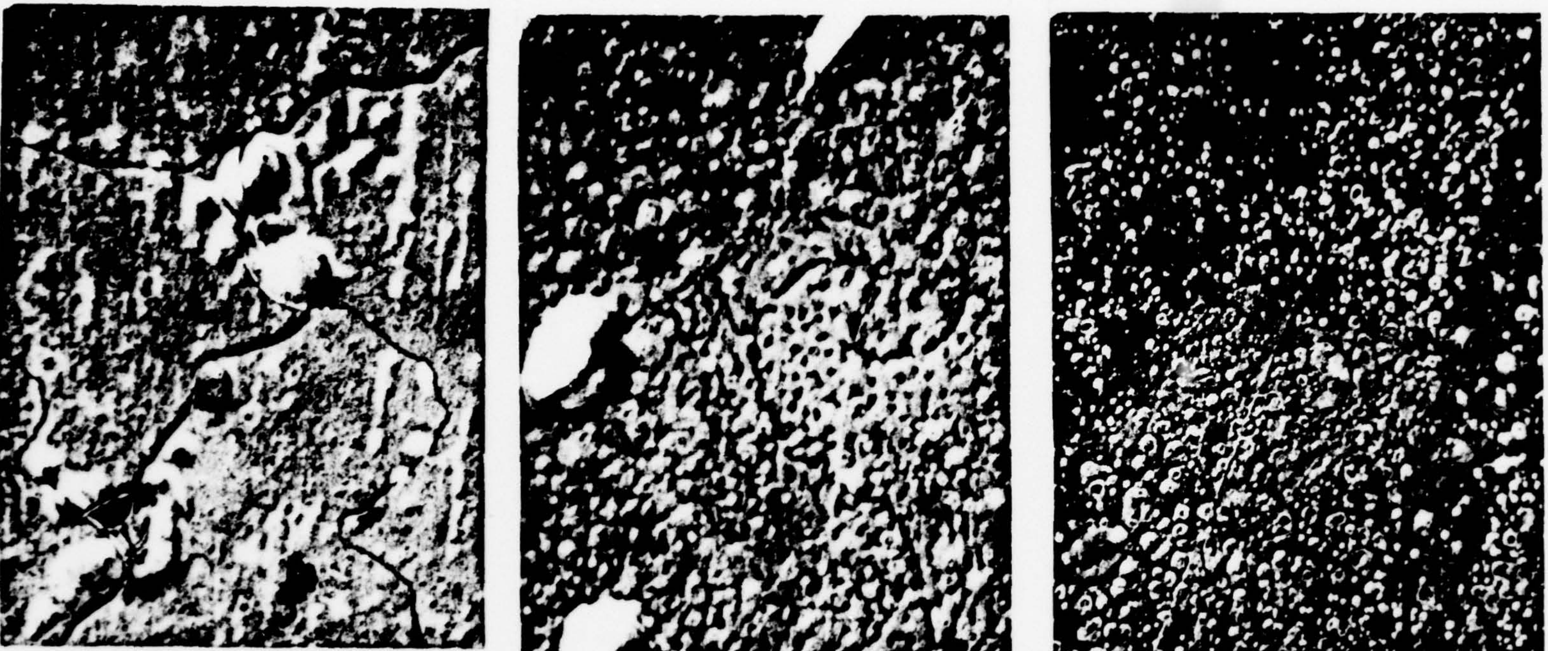

a) (100) b) (110) c) (111)

Figure 9. SiO ($\lambda/4$) on CaF_2. Typical HF Vapor Damage on Three Substrate Orientatations. 60 Min. 167X.

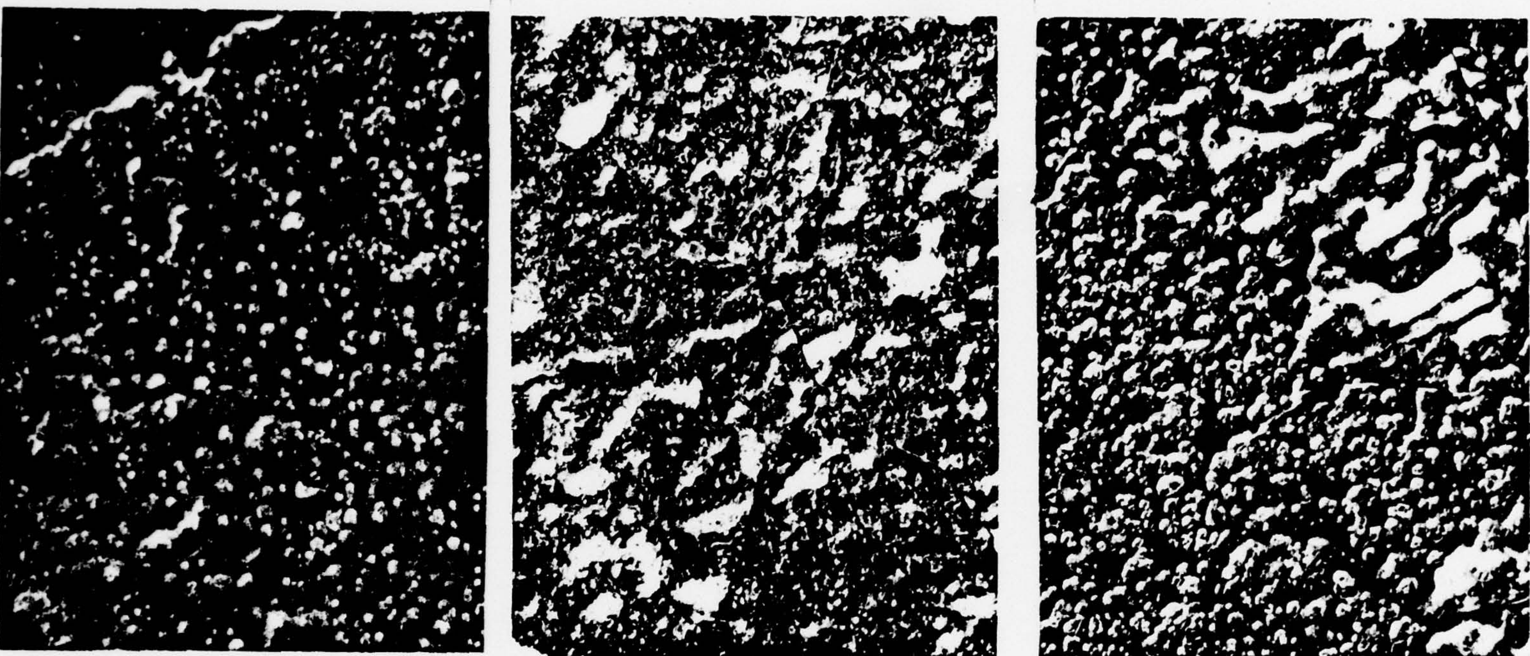

a) (100) b) (110) c) (111)

Figure 10. SiO (λ/4) on SrF_2. Typical HF Vapor Damage on Three Substrate Orientations. 167X.

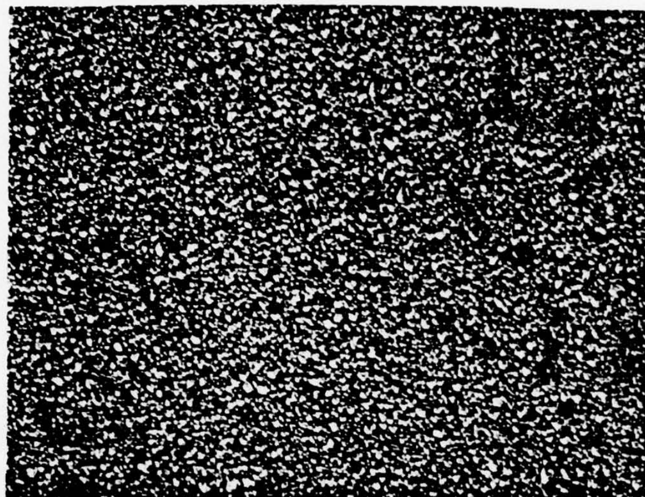

a) CaF_2 (111) Substrate.

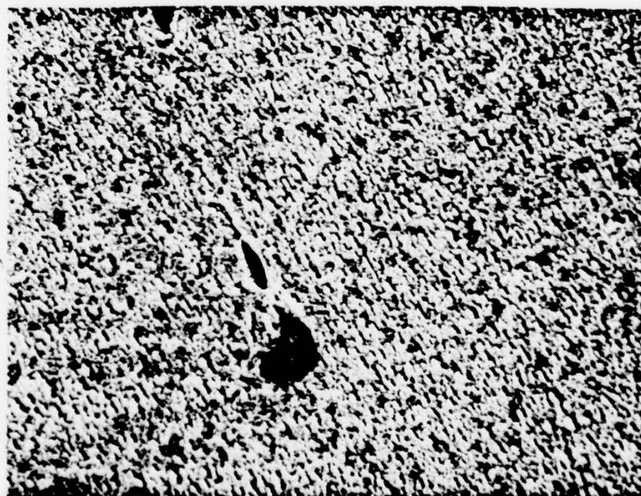

b) SrF_2 (111) Substrate.

Figure 11. ZnS ($\lambda/4$) Films. Typical HF Damage 30 Min. 167X.

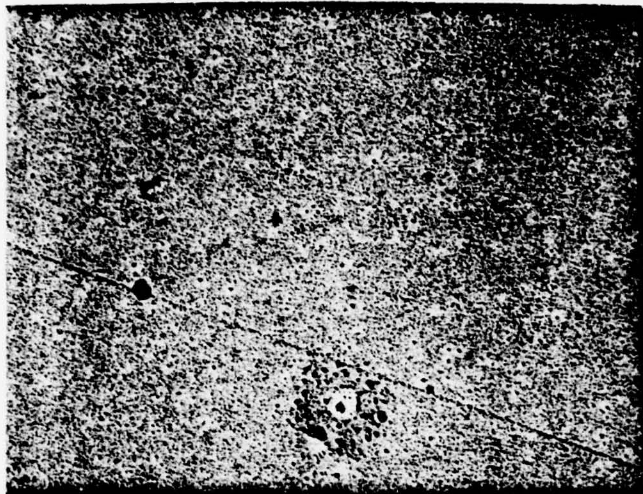

a) CaF_2 (110) Substrate.

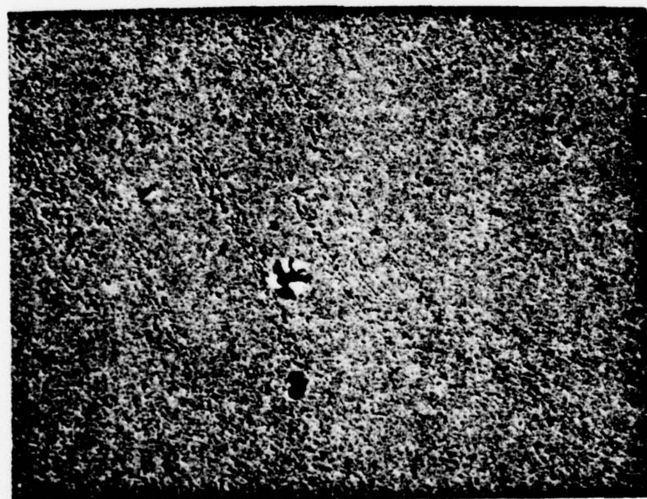

b) SrF_2 (110) Substrate.

Figure 12. ZnSe (λ/4) Films. Typical HF Damage 15 Min. 167X.

3.0 MULTILAYER ANTIREFLECTION COATINGS.

The intended application of most of the thin film material properties generated under this program is in the design of multilayer coatings for use on laser optics. In such multilayer applications, the surface encountered by the depositing material of the layer nearest the substrate is essentially identical to that in the single layer case, from which properties and structure were determined. The depositing material of the second layer (and any succeeding layers) encounters the surface of the first coating as its substrate, giving rise to possible differences in coating structure or properties. Thus it is necessary to determine absorptance and coating structure for multilayer coatings to establish similarities and differences in behavior in comparison with single layer coatings.

3.1 Absorptance of Multi Layer Coatings

Absorptance values for coatings on window samples coated on both sides with a quarterwave-quarterwave design composed of ThF_4 and either PbF_2 or SiO are listed in Table IV for the DF laser wavelength region. The absorptance of the substrates ($\sim 1 \times 10^{-4}$) has been subtracted out in all cases so that the tabulated numbers represent the absorptance of two (2) coated surfaces. Mean values for each coating/substrate combination are listed at the far right; mean values for each coating pair and substrate orientation are also given for purposes of comparison.

Some general observations to be drawn from the data include the relatively high absorptance and strong variation with substrate orientation of the ThF_4/PbF_2 coatings as compared to ThF_4/SiO and the small differences between average values for a given coating pair on CaF_2 or SrF_2 substrates. The last observation is in accord with single layer data as is the stronger

Table IV. Absorptance of Antireflection Coatings on Single Crystal CaF_2 and SrF_2 Substrates (2 coated surfaces) at 3.8 μm.

Materials & Design	Coating Absorptance for Various Substrate Orientations ($\times 10^4$).			Mean Coating Absorptance
	(100)	(110)	(111)	($\times 10^4$)
ThF_4/PbF_2 on CaF_2	9.62	7.00	7.48	8.03
ThF_4/PbF_2 on SrF_2	9.30	5.54	7.15	7.33
ThF_4/PbF_2 Mean	9.45	6.27	7.32	7.68
ThF_4/SiO on CaF_2	4.30	3.60	3.12	3.67
ThF_4/SiO on SrF_2	3.60	4.00	3.44	3.68
ThF_4/SiO Mean	3.95	3.80	3.28	3.68

variation with substrate orientation. The lower mean absorptance of the ThF_4/SiO pair as compared to the ThF_4/PbF_2 pair is also in accord with single layer data, but the difference is much more pronounced. In the single layer case the difference amounts to only 10 to 20%, depending upon whether the absorptance values are those for halfwave coatings only or were determined as a function of coating thickness (3L vs. L). For the present set of antireflection coatings the difference in mean absorptance between the two designs is almost exactly a factor of two. This last observation is generally not in accord with experience on the LWTVP program, where differences between the same two coating designs averaged less than 10%, over a large number of single and polycrystalline substrates of CaF_2 and SrF_2.

Comparing the overall magnitude of the AR coating absorptances in Table IV with averages for the LWTVP program reveals that the present results for ThF_4/PbF_2 are consistently higher than the former results by a factor of four; those for ThF_4/SiO are higher by a factor of two in the present case. Overall agreement between single layer absorptance results for ThF_4 and PbF_2 and AR results for the pair obtained under the present program is within 10%, the single layer results being higher. Single layer absorption coefficients for ThF_4 and SiO lead to a calculated mean absorptance for the AR coating which is about double the actual measured value obtained under the present program.

These problems, taken together with the inconsistencies in the results of the absorptance vs. film thickness studies for ThF_4 indicate strongly that the raw materials presently available from Balzers and Cerac differ from those purchased in the initial phase of the LWTVP program. Impurities such as oxides, oxyfluorides, or hydrated fluorides of Thorium would increase the absolute level of absorptance in coating designs involving ThF_4 and could lead to inconsistencies in absorptance based on interaction of these impurities with other coating materials in a multilayer design.

Comparison of mean absorptance of ThF_4/PbF_2 antireflection coatings on polycrystalline CaF_2 (8.91×10^{-4} for two coated surfaces) with the mean for the same pair on three orientations of single crystal CaF_2 substrates (Table IV) shows a difference of only 10%, with the polycrystalline substrate values being higher. Comparison of the coating absorptance on polycrystalline substrates with the mean calculated value using single layer (halfwave) data (9.60×10^{-4} for two coated surfaces) shows a difference of 7.5%, with the single layer calculated value being the higher. Thus, it appears that both the single layer and multilayer coating absorptances have practical value in predicting performance of coatings in systems of interest for real devices. However, much work is still required to achieve higher degrees of correlation and to understand the underlying phenomena responsible for the results.

3.2 Structure and Preferred Orientation in Multilayer Coatings.

In order to ascertain whether differences in coating structure or preferred orientation in multilayer and single layer coatings are associated with observed differences in coating absorptance, both coating pairs (ThF_4/PbF_2 and ThF_4/SiO) were subjected to x-ray diffraction analysis on all three single crystal substrate orientations. Results of these analyses are summarized in Tables V and VI, for ThF_4/PbF_2 and ThF_4/SiO, respectively.

Considering first the results in Table V for ThF_4/PbF_2, we see that the structure and preferred orientation of the PbF_2 component film of the two-layer pair (deposited first on the uncoated substrate surface) is similar in most respects to that of the single layer film on a similarly oriented substrate (compare with Technical Report of September, 1977). The only major difference is the presence of a considerable amount of (100) oriented PbF_2 on (100) CaF_2, in addition to the (111) oriented PbF_2 which was the predominant orientation in the single layer case on (100) CaF_2. All other

differences in the PbF_2 structure and orientation on CaF_2 or SrF_2 are quite minor, involving presence or absence of the orthorhombic α-phase (a minor constituent) or details of its preferred orientation.

On the other hand, the ThF_4 component film of the ThF_4/PbF_2 pair, which is deposited on top of the PbF_2 film in the AR coating, shows very little similarity of structure or preferred orientation with the single layer ThF_4 films deposited on the bare substrate. On (100) CaF_2, the ThF_4 component film is crystalline with a predominant (110) preferred orientation; single layer films (quarterwave or halfwave) on corresponding substrates were crystalline with a (270) ≅ (213) preferred orientation. On (110) CaF_2 substrates, the ThF_4 film of the AR coating is microcrystalline as in the single layer case, but with subequal (110) and $(32\bar{1})$ preferred orientation. The single layer films had subequal (110) and (103) orientation. On (111) CaF_2, the ThF_4 in the AR coating is well crystallized with a (110) preferred orientation, whereas the single layer films exhibit a strong $(32\bar{1})$ orientation. On SrF_2 substrates the ThF_4 of the AR coating is amorphous to x-ray on (100) and (111); single layer films on SrF_2 substrates of these orientations were microcrystalline and well crystallized with strong (010)/(322) orientation, respectively. The structure and orientation of ThF_4 films on (110) SrF_2 is similar in both the ThF_4/PbF_2 coating and the single layer film, having a strong $(52\bar{1})$ orientation with minor amounts of less strongly oriented material.

Structure and preferred orientation of component films of the ThF_4/SiO pair (Table VI) is similar to the single layer films in four of the six substrate/coating combinations studied here. On (100) CaF_2 both SiO and ThF_4 are amorphous to x-ray. For SiO, this structure is similar to the single layer case; for ThF_4, the single layer films on this substrate orientation had been consistently crystalline with strong, subequal (270) and $(21\bar{3})$

Table V. Summary of Structures and Preferred Orientation in Component Films of the ThF_4/PbF_2 Quarterwave-Quarterwave Coating on CaF_2 and SrF_2 Substrates.

Substrate Material	Substrate Orient.	PbF_2 Structure and Orientation	ThF_4 Structure and Orientation
CaF_2	(100)	β(cubic) (100) $\geq$ (111) α (orthorh) (012)	Monoclinic, (110) > $(44\bar{3})$
	(110)	β (110) ; α (100)	Microcrystalline, (110) $\cong$ $(32\bar{1})$
	(111)	β (111) , Minor (110) α (001)	Monoclinic (110) ; Minor μcryst.
SrF_2	(100)	β (100) ; Minor α (012) > (035).	Amorphous to X-Ray.
	(110)	β (110).	Monoclinic $(52\bar{1})$ > $(43\bar{1})$
	(111)	β (111)	Amorphous to X-Ray.

Table VI. Summary of Structures and Preferred Orientation in Component Films of the ThF_4/SiO Quarterwave-Quarterwave Coating on CaF_2 and SrF_2 Substrates.

Substrate Material	Substrate Orient.	SiO Structure and Orientation	ThF_4 Structure and Orientation
CaF_2	(100)	Amorphous to X-Ray	Amorphous to X-Ray
	(110)	Amorphous/Microcrystalline SiO_2 (α-Quartz) (100)	Microcrystalline, Monoclinic (110) + $ThF_4 \cdot nH_2O$ (211).
	(111)	Crystalline, α-Quartz (311) + Minor Tridymite (105)	Crystalline, Monoclinic $(32\bar{1})$, Minor (332).
SrF_2	(100)	Amorphous/Microcrystalline	Crystalline, Monoclinic (252)
	(110)	Amorphous to X-Ray	Microcrystalline, Monoclinic (102)
	(111)	Crystalline, α-Qtz. (110) + Microcrystalline (6.30Å)	Crystalline, Monoclinic (322)

preferred orientations. On (110) CaF_2, the structure and orientation of both films of the pair is similar to the single layer case; the only significant difference is the presence of a diffraction peak attributable to the (211) spacing of $ThF_4 \cdot nH_2O$[2] in the two-layer coating. On (111) CaF_2, SiO is crystalline with α-quartz and minor tridymite; in the single layer case it was amorphous or microcrystalline. The ThF_4 structure and preferred orientation in the multilayer and single layer films on (111) CaF_2 are essentially identical.

On (100) SrF_2, SiO and ThF_4 films of the multilayer coating have structure and orientation similar to single layer films of the same materials. The only notable difference is the absence of diffraction peaks attributable to hydrated ThF_4 in the multilayer case. On (110) SrF_2 the structure and orientation of both SiO and ThF_4 differ from the single layer cases with SiO being amorphous rather than crystalline or microcrystalline and ThF_4 being microcrystalline with a (102) preferred orientation rather than crystalline with a strong $(52\bar{1})$ orientation, as in the single layer case. Finally, on (111) SrF_2, SiO and ThF_4 component films are both crystalline, as in the single layer case. However, the SiO yields diffraction peaks for α-Quartz and some microcrystalline material with spacings near 6.30Å, rather than for Tridymite, as in the single layer case. The ThF_4 of the multilayer coating has a (322) preferred orientation, as compared to the (010) orientation of single layer films. In addition, no diffraction peaks attributable to hydrated ThF_4 are evident in the multilayer case, whereas a minor peak was observed in the single layer case.

In summary of the multilayer coating structure and orientation results, it appears that the PbF_2 structures are nearly identical to the single layer films in all cases, which is exactly as expected. Although the structure and orientation of the ThF_4 films of the ThF_4/PbF_2 coating pair differed

from the single layer films in most cases, it is apparent that these differences did not significantly affect absorption, as noted in the previous subsection. In the ThF_4/SiO pair on the other hand, differences in both the SiO and ThF_4 film structures were observed, on comparison with the single layer cases. The absence of hydrated ThF_4 material in the multilayer case is significant and may explain the markedly reduced absorption in comparison with the single layer films. The differences in the SiO component of the multilayer are in the direction of less crystallinity and identification of α-quartz rather than Tridymite as the crystalline SiO_2 phase, when SiO_2 is present. These characteristics are difficult to identify with reduced absorptance at 3.8 μm, except that it is possible the multilayer films are less rich in oxygen than was the case with the single layer films.

4.0 REFERENCES.

1. ASTM Powder Diffraction File Card No. 23-1426.
2. ASTM Powder Diffraction File Card No. 9-304.
3. ASTM Powder Diffraction File Card No. 12-96.
4. ASTM Powder Diffraction File Card No. 2-29.